ANALYSIS OF BASE ISOLATED LIQUID STORAGE TANKS WITH 3D FSI-ANALYSIS AS WELL AS SIMPLIFIED APPROACHES

J. Rosin[1], K. Mykoniou[2], C. Butenweg[3]

[1] *Project Engineer, Chair of Structural Analysis and Dynamics, RWTH Aachen University, Germany & SDA-engineering GmbH, Herzogenrath, Germany, rosin@sda-engineering.de*

[2] *Project Engineer, Chair of Structural Analysis and Dynamics, RWTH Aachen University, Germany & Bridge Design Services AG, Zurich, Switzerland, konstantinos.mykoniou@bds-ag.ch*

[3] *Professor, Institute of Mechanics and Structural Engineering, University of Applied Science Aachen, Germany &SDA-engineering GmbH, Herzogenrath, Germany, christoph.butenweg@fh-aachen.de*

Abstract

Tanks are preferably designed, for cost-saving reasons, as circular, cylindrical, thin-walled shells. In case of seismic excitation, these constructions are highly vulnerable to stability failures. An earthquake-resistant design of rigidly supported tanks for high seismic loading demands, however, uneconomic wall thicknesses. A cost-effective alternative can be provided by base isolation systems. In this paper, a simplified seismic design procedure for base isolated tanks is introduced, by appropriately modifying the standard mechanical model for flexible, rigidly supported tanks. The non-linear behavior of conventional base isolation systems becomes an integral part of a proposed simplified process, which enables the assessment of the reduced hydrodynamic forces acting on the tank walls and the corresponding stress distribution. The impulsive and convective actions of the liquid are taken into account. The validity of this approach is evaluated by employing a non-linear fluid-structure interaction algorithm of finite element method. Special focus is placed on the boundary conditions imposed from the base isolation and the resulting hydrodynamic pressures. Both horizontal and vertical component of ground motion are considered in order to study the principal effects of the base isolation on the pressure distribution of the tank walls. The induced rocking effects associated with elastomeric bearings are discussed. The results manifest that base isolated tanks can be designed for seismic loads by means of the proposed procedure with sufficient accuracy, allowing to dispense with numerically expensive techniques.

Keywords: liquid storage tank; seismic isolation; elastomeric bearing; friction pendulum bearing; simplified approach

1. Introduction

Liquid storage tanks are important lifeline structures since they have substantial use in industrial facilities, nuclear power plants and infrastructure. The tank structure is usually designed as circular cylindrical shell, because this geometry is able to carry the hydrostatic pressure from the liquid filling with a minimum of material. This leads to thin-walled constructions, which are highly vulnerable to stability failures in case of seismic excitation. Instead of increasing the wall thickness an earthquake protection system can be an effective alternative to ensure the stability. The idea of seismic isolation consists in reducing the peak response of the tank through implementation of isolation devices between the tank base and the foundation. Definitely, the concept of isolating structures from the damaging effects of earthquake is not new. A detailed review of recent works in base isolation systems and their application to buildings can be found in Kelly [1] or Mayes and Naeim [2]. Nevertheless, the response of liquid storage tanks to seismic excitation differs from that of building structures and is quite complex, since the dynamic interaction effects between tank wall and liquid must be considered. Different simplified approaches for the calculation of seismically excited anchored tank structures can be found in the literature. However, these approaches are based on the assumption of a rigidly supported tank bottom and they are not applicable to base isolated tanks, because of the nonlinear behavior of the seismic isolation and the combined modes of vibrations of tank and fluid. To capture those complexities, a highly sophisticated fluid-structure interaction model has to be set up for a realistic simulation of the overall dynamic system.

In recent past, a large number of theoretical and experimental studies have been made on isolation of liquid storage tanks with different base isolation systems. Panchal and Soni [3] present an state-of-the-art-review on isolated liquid storage tanks with focus on analytical and experimental studies conducted on tanks. It can be recognized that, so far, the responses of seismically isolated tanks have been studied by means of elaborated fluid-structure-interaction models in only very few works. On the contrary, the calculations are limited to mechanical models, with which the influence of seismic isolation to the foundation load (shear force and overturning moment), the displacements above the insulating plane and the sloshing of the fluid surface is determined. By using these models, the calculation of the exact reduction of the hydrodynamic pressure - and accordingly of the stresses in the tank shell - is not possible. Additionally, the nonlinear characteristics of the isolation system are frequently neglected for reasons of simplification, as well as aspects such as tensile load of the isolation systems or rocking of the tank structure have not been studied. However, no general accepted calculation concept exists. Therefore, the aims of this study are as follows: (i) To propose a simplified calculation method for anchored liquid storage tanks according to the state of the art; (ii) to investigate the overall seismic behavior isolated tanks with a complex fluid-structure-interaction model and (iii) to propose a simplified analysis for evaluation of the seismic response of base-isolated tanks based on the method of (i) and the results of (ii).

2. Calculation of anchored liquid storage tanks

The seismic response of tanks is quite different from conventional buildings first of all due to the hydrodynamic effects. The hydrodynamic pressures and the resultant stresses depend on the characteristics of the seismic motion, the properties of the liquid and the flexibility of the tank shell [4]. The latter one introduces the necessity to solve a fluid-structure-interaction problem since the magnitude and distribution of the pressure and the associated tank forces are strongly influenced by the stiffness of the tank. Two approaches are distinguished: the added mass formulation and finite element formulations for the fluid. In the added mass approach, the governing equations of the fluid are used to transform the pressures applied to the structure in an equivalent virtual mass added on the structural modal. This procedure is highly desirable since it reduces the spatial dimensionality of the fluid-structure-interaction problem by one: the three-dimensional governing partial differential equations for the fluid flow are transformed into the wall-surface integral equations. Unfortunately, the added mass concept cannot replicate the actual physical behavior of liquid storage tanks when the tank exhibits nonlinear behavior or a support deviating from the rigid support. For this case, finite element formulations for the fluid are proven to be appropriate. Here, within a three dimensional model the tank structure as well as the fluid is part of a complex fluid-structure-interaction (FSI) model. Special contact elements consider their interaction during a time history calculation. Since such a model is extremely complex and the software capabilities allow such calculations only in recent years at all, the added mass concept usually comes into use for design purposes. The design of liquid storage tanks according to this concept has motivated systematic research efforts over the last decades. Veletsos [5], Haroun and Housner [4] Fischer et al. [6], Malhotra et al. [7] and Meskouris et al. [8] may be mentioned as representative literature. In the following, a proposal for a simplified design process according to the added mass concept and the current state of the art [4], [5], [6], [7], [9] is introduced, which enables the calculation of hydrodynamic pressures exerted on anchored liquid storage tanks due to ground motion.

According to a well-established concept, the hydrodynamic pressure components can be determined as the sum of two parts: an impulsive part $\bar{p}_i$ which represents the action of the part of the liquid which moves in unison with the tank shell and a convective part $\bar{p}_c$, which represents the action of the part of the liquid that experiences sloshing motion. The dynamic interaction between the two parts is traditionally neglected. Since the oscillation periods of the two parts are far apart, each mode of oscillation with its associated pressure distribution can be determined individually. With regard to the Eigenfrequencies of the individual oscillation components, site response spectra can be used to determine the spectral acceleration of the modes.

The following formulas are based on a thin-walled circular cylindrical shell of height L, radius R and uniform wall thickness s (Fig. 1). The shell is assumed to be steel with Young's modulus E, Poisson ratio ν and mass density ρ. The bottom of the shell is regarded as flat, rigid and anchored to the ground. The tank is filled to the height H with a non-viscous, irrotational and incompressible liquid of mass density ρ_L. In Fig. 1, ξ and ζ are

the dimensionless coordinates for radius ($\xi = r/R$) and wetted height of the tank wall ($\zeta = z/H$) and θ is the peripheral angle.
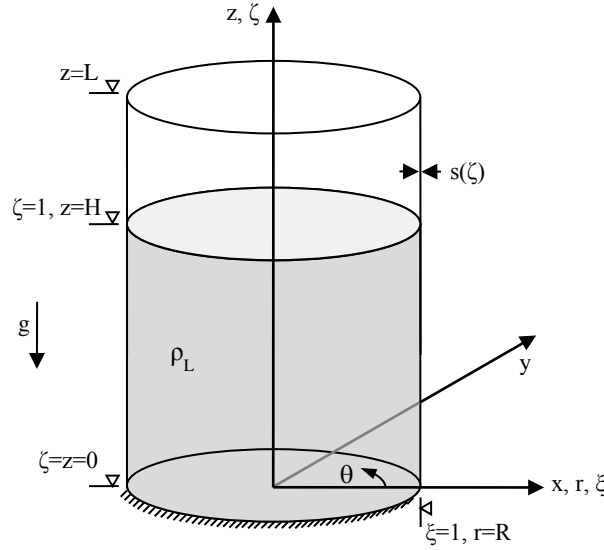

Fig. 1 – Geometry of the system under investigation

2.1 Horizontal seismic excitation

For practical applications, only the first sloshing mode and the first and second radial mode of vibration (index n in Eq. (1)) needs to be considered [7], [8]. It is assumed that only the first circumferential mode of vibration is activated. The total maximum dynamic wall pressure p_h then can be computed as:

$$p_h\,(\xi = 1, \zeta, \theta) = \rho_L \cdot R \cdot \cos(\theta) \sqrt{\left[\bar{p}_{c,1}(\xi = 1, \zeta) \cdot S_{a,c,1}^{abs}\right]^2 + \sum_{n=1}^{2}\left[\bar{p}_{i,n}(\xi = 1, \zeta) \cdot S_{a,i,n}^{abs.}\right]^2} \tag{1}$$

In Eq. (1), $S_{a,c,1}^{abs}$ and $S_{a,i,n}^{abs}$ denote the absolute spectral acceleration of the horizontal site spectra corresponding to the sloshing frequency and the frequencies of the impulsive modes of respectively. According to [6], [8], [9], the damping rates of the site spectra are 0,5% for the sloshing mode and 2,5% for the impulsive modes. The sloshing frequency $\omega_{c,1}$ of the first sloshing mode can be obtained e.g. from Fischer et al. [6] with:

$$\omega_{c,1} = \frac{g}{R} \cdot 1{,}841 \cdot \tanh\left(1{,}841 \cdot \frac{H}{R}\right) \tag{2}$$

The normalized wall pressure distributions $\bar{p}_{c,1}$ can be computed according to [6] by:

$$\bar{p}_{c,1}(\xi = 1, \zeta) = 0{,}837 \cdot \frac{\cosh\left(1{,}841 \cdot \frac{H}{R} \cdot \zeta\right)}{\cosh\left(1{,}841 \cdot \frac{H}{R}\right)} \tag{3}$$

For fully filled tanks, the natural circular frequencies of the shell-liquid vibration can be calculated as a function of the slenderness ratio H/R and the thickness ratio s/R according to the expression [10]:

$$\omega_{i,n} = \frac{C_{1,n}}{H} \cdot \sqrt{\frac{E \cdot \rho_L}{\rho \cdot \rho_W}}, \quad n = 1,2,3 \tag{4}$$

Here, ρ_W is the mass density of water. The coefficients $C_{1,n}$ for the first and second axial mode are given by:

$$C_{1,1} = 0{,}14 \cdot \left(\frac{s}{R}\right)^{0,48} \cdot \left(\frac{H}{R}\right)^3 - \left(\frac{s}{R}\right)^{0,48} \cdot \left(\frac{H}{R}\right)^2 + 1{,}93 \cdot \left(\frac{s}{R}\right)^{0,47} \cdot \frac{H}{R} + 1{,}76 \cdot \left(\frac{s}{R}\right)^{0,54} \tag{5}$$

$$C_{1,2} = \left[1{,}85 \cdot \ln\left(\frac{H}{R}\right) + 5{,}25\right] \cdot \left(\frac{s}{R}\right)^{0,5} \tag{6}$$

The above expressions are, strictly speaking, applicable for thin tanks $R/s \geq 200$ without roof and uniform wall thickness. The normalized wall pressure distributions $\bar{p}_{i,n}$ of tanks with slenderness ratios $0.3 \leq H/R \leq 3$ are given in Tab 1. The values presented correspond to steel tanks of uniform thickness ratio $s/R = 1000$. Nevertheless, there are also valid for other thickness ratios, since the pressure distribution is practically independent of the wall thickness apart from concrete tanks. For tanks with non-uniform thickness of the tank wall, s can be calculated by taking a weighted average over the height assigning the highest weight near the base of the tank [7]. For slenderness ratios apart from those in Tab. 1 the values can be found by interpolation.

Table 1 – Design normalized wall pressure distributions [10]

| | $\bar{p}_{i,1}$ | | | | | | $\bar{p}_{i,2}$ | | | | | |
| | H/R | | | | | | H/R | | | | | |
ζ	0,5	1,0	1,5	2,0	2,5	3	0,5	1,0	1,5	2,0	2,5	3
0	0,3826	0,6391	0,6342	0,5341	0,4295	0,3421	0,0106	0,0406	0,1779	0,3024	0,3654	0,3729
0,1	0,4060	0,6712	0,6724	0,5788	0,4791	0,3943	0,0121	0,0436	0,1868	0,3197	0,3956	0,4185
0,2	0,4139	0,6857	0,7155	0,6480	0,5661	0,4916	0,0110	0,0369	0,1640	0,2948	0,3883	0,4410
0,3	0,4030	0,6877	0,7566	0,7264	0,6707	0,6127	0,0069	0,0243	0,1193	0,2331	0,3336	0,4103
0,4	0,3795	0,6734	0,7852	0,7985	0,7756	0,7400	0,0012	0,0084	0,0605	0,1421	0,2318	0,3159
0,5	0,3441	0,6394	0,7914	0,8501	0,8645	0,8568	-0,0047	-0,0076	-0,0018	0,0371	0,0985	0,1696
0,6	0,2971	0,5822	0,7656	0,8664	0,9194	0,9440	-0,0092	-0,0205	-0,0558	-0,0618	-0,0405	-0,0002
0,7	0,2392	0,4984	0,6975	0,8303	0,9180	0,9762	-0,0113	-0,0276	-0,0905	-0,1339	-0,1542	-0,1542
0,8	0,1712	0,3834	0,5737	0,7188	0,8289	0,9135	-0,0103	-0,0272	-0,0975	-0,1603	-0,2106	-0,2471
0,9	0,0929	0,2301	0,3720	0,4932	0,5951	0,6822	-0,0064	-0,0185	-0,0714	-0,1260	-0,1800	-0,2308
1	0	0	0	0	0	0	0	0	0	0	0	0

2.2 Vertical seismic excitation

For tanks with walls free to move in the radial direction at the bottom and top edges, the deformation figure is described by a cosine curve. In this case and by neglecting the wall mass, the fundamental natural frequency can be obtained in closed form [11]:

$$\omega_{0,1} = \frac{1}{R} \cdot \sqrt{\frac{\pi \cdot E \cdot s \cdot I_1\left(\frac{\pi}{2 \cdot H/R}\right)}{H \cdot \rho_L \cdot (1 - \nu^2) \cdot I_0\left(\frac{\pi}{2 \cdot H/R}\right)}} \tag{7}$$

This expression with the modified Bessel function I_1 and I_0 was also adopted in the European standard Eurocode 8 [9]. Tang [12] also manifested that the hydrodynamic effects of vertically excited tanks are insensitive to the condition of the support at the tank base. For design purposes, the total maximum dynamic wall pressure can be computed by the following expression:

$$p_v\,(\xi = 1, \zeta) = H \cdot \rho_L \cdot (1 - \zeta) \cdot S_{a,v,1}^{abs.} \tag{8}$$

It is important to note that, although the higher modes of vibration do not appear explicitly in Eq. (10), the contributions of them are accounted by approximately using the distribution function corresponding to a rigid tank and the absolute spectral acceleration of the fundamental mode.

3. Base isolation of liquid storage tanks

In the event of strong earthquakes tank structures are subjected to high loads due to the impulsive hydrodynamic pressure. Typical tank structures are designed with height/radius ratios of around $0.5 \leq H/R \leq 3$ and radius/tank wall thickness ratios of around $500 \leq R/s \leq 1000$. For tank structures within this field of geometry and a liquid filling with a density similar to water the impulsive vibration mode is attended by oscillation periods of about 0,1 to 0,2 seconds according to Eq. (4) and thereby attended by the maximum spectral acceleration of common response spectra. Here, a base isolated support has two important advantages: On the one hand, an elongation of the oscillation period, which leads to a reduction of the spectral acceleration. On the other hand, the base isolation system dissipates seismic energy and the spectral acceleration is consequently decreased.
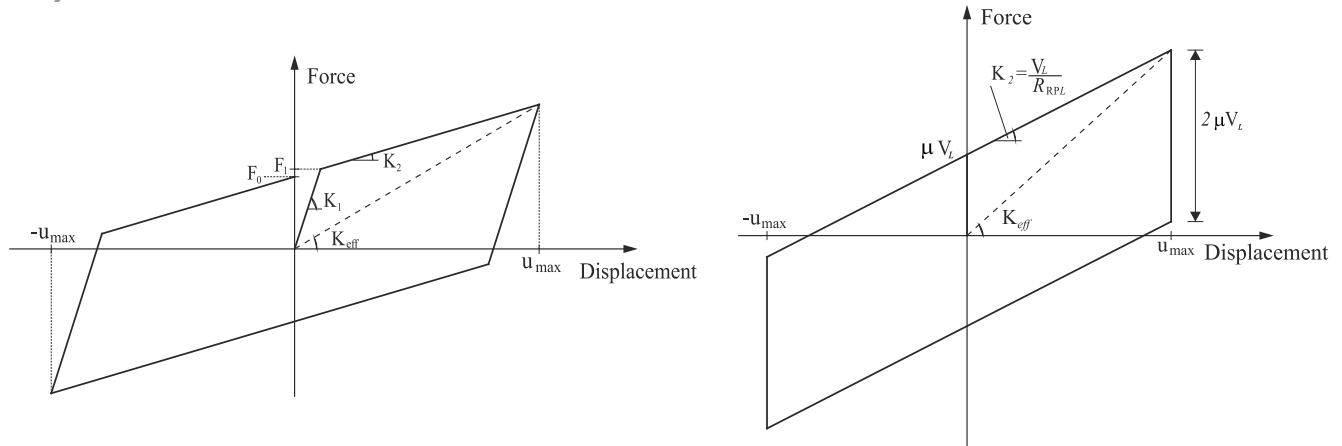
Fig. 2 – Idealized bilinear hysteresis for modeling of an elastomeric bearing (left) and friction pendulum bearing (right)

Mostly, elastomeric bearings with lead core or friction pendulum bearings are used for the seismic isolation of tank structures worldwide. The cyclical behavior of these types of isolation can be idealized by means of their force-deflection curve, the hysteresis curve. The hysteresis curve of both bearings can be approximated bilinear.

3.1 Elastomeric bearings with lead core

The hysteresis can be constructed by superposition of the force-deformation curves of lead core and elastomer and is shown in Fig. 2. In the elastic range, the sum of the stiffness of the lead core and the stiffness of the elastomer gives the elastic stiffness K_1 of the bearing. However, this is difficult to detect, so K_1 is usually given by a proportion of the horizontal stiffness after reaching the yield strength: $K_1 = \beta \cdot K_2$ (proportionality factor β_K: 10 ~ 15 [2]). The stiffness K_2 results from the stiffness of the elastomer:

$$K_2 = \frac{G_{El} \cdot A_{El}}{H_L} \tag{9}$$

Here, G_{El} stands for the shear modulus, A_{El} the area of the elastomer and H_L the height of the bearing. The characteristic force F_0 of the hysteresis corresponds approximately to the yield limit of the lead core. The reader should not confuse this force with the yield force F_1 of the entire bearing, which is given with

$$F_1 = F_0 + K_2 \cdot u_y \tag{10}$$

with u_y being the horizontal displacement of the bearing in the transition from the elastic in the plastic range. Basically, the plastic deformation ability of the lead core determines the damping capacity of the bearing.

3.2 Friction pendulum bearings

The biaxial hysteretic behavior of a single friction pendulum, is shown in Fig. 2. The initial friction force is given in dependence of the friction coefficient μ and the vertical load of the bearing V_L by

$$F_0 = \mu \cdot V_L \tag{11}$$

After exceeding the initial friction force F_0 and the corresponding horizontal relative displacement u_y, an upward movement of the upper bearing plate follows the horizontal displacement u due to the concave sliding surface of the bearing, whereby a vertically directed force is activated. The vertical force depends on the curvature of the sliding surface R_L and increases in proportion to the horizontal displacement. The restoring force of the bearing can then be calculated:

$$F_L = \frac{V_L}{R_L} \cdot u + \mu \cdot V_L \cdot sign\left(\dot{u}\right) \tag{12}$$

The friction force opposes the sliding direction, which is ensured by the use of signum function $sign\,(\dot{u})$. With these relations the hysteresis is approximated:

$$K_1 = \frac{V_L \cdot \mu}{u_y} + K_2 = \frac{V_L \cdot \mu}{u_y} + \frac{V_L}{R_L} \tag{13}$$

3.3 Calculation with a fluid-structure-interaction model

In order to evaluate the seismic response of an isolated liquid storage tank within an FSI-analysis, the general purpose finite element code LS-DYNA© is used. LS-DYNA© is capable of handling all complexities related to seismic excited liquid storage tanks. For example, Ozdemir et al. [13] and Maekawa [14] had good experiences with LS-DYNA© concerning the simulation of anchored tanks. The software provides an explicit time marching scheme based on the central difference method, which offers advantages, especially for the solution of dynamic contact problems. Due to the superiorities of the Arbitrary Lagrangian Eulerian (ALE) formulation over Lagrangian method, the interaction effects between fluid and structure are modeled using the ALE method. Both material and geometric nonlinearities are considered. The general modeling follows the recommendations from Ozdemir et al. [13] and is described in [15]. Here, detailed focus is set on the implementation of base isolation systems.

There are basically two options for the finite element modeling of a seismic isolation. Firstly, a specific 3D model of a bearing can be created, which accurately reproduces bearings according to their geometry and their material. Alternatively, there is the possibility of a discrete modeling through the use of spring elements, which are placed between two nodes. These elements can be associated with a corresponding nonlinear material model that represents the mechanical properties of the seismic isolation. Here, the focus is not given to the behavior of the seismic isolation but to the reaction of the isolated tank, so the discrete modeling is performed. Concretely, friction pendulum bearings with spherical or cylindrical sliding surface and elastomeric bearings are modeled on the basis of bi-directional coupled plasticity theory. In LS-DYNA© a specific material model is available. The hysteretic behavior was proposed by Bouc [16] and Wen [17]. The sliding bearing behavior is described in detail in the work of Constantinou [18].

In the context of a forced single degree of freedom hysteretic oscillator, the equation of motion using the Bouc-Wen model is:

$$m \cdot \ddot{u} + c \cdot \dot{u} + \beta_k \cdot k \cdot u + (1 - \beta_k) \cdot k \cdot z = f \tag{14}$$

where m, c, k, f and β_k are the mass, damping coefficient, stiffness, external excitation and plastic to elastic stiffness ratio respectively. The hysteretic ausxiliary variable z, according to the Bouc-Wen model is given by:

$$u_0 \cdot \dot{z} + \gamma \cdot |\dot{u}| \cdot |z| \cdot |z|^{\eta-1} + \beta \cdot |\dot{u}| \cdot |z|^{\eta} - A \cdot \dot{u} = 0 \tag{15}$$

Therein, u_0 is the initial displacement while η the transition into the inelastic range controls. z can be considered as continuous approximation of the signum function $sign(\dot{u})$. Extensive studies manifested that values of $\eta = 2$ with $A = 1$ and $\beta + \gamma = 1$ ($\beta = 0.1$; $\gamma = 0.9$) generate force-deflection curves in good agreement with experimental data [18], [19].

While for elastomeric bearings the ratio of plastic to elastic stiffness is given as a material property, for friction pendulum bearings this ratio is derived from the geometry and friction properties. Therefore, in LS-DYNA© specification of the radii of the sliding surface in the x- and y-direction is required. The friction coefficient depends on the bearing pressure and on the sliding velocity of the bearing v_{rel}. The following equation is used:

$$\mu = \mu_{dyn} + \left(\mu_{stat} - \mu_{dyn}\right) \cdot e^{-D|v_{rel}|} \tag{16}$$

where μ_{dyn} is the coefficient of friction at large velocity of sliding and μ_{stat} the one at very low velocity. D is a constant for given bearing pressure and condition of the interface. Usually, these values are experimental data.

Other input parameters for both types of bearings are their mass vertical stiffness. In addition, a damping of free vertical vibrations due to the dead weight of the bearing and its vertical stiffness can be defined.

The FSI-model is used for a parametric study with different tank geometries and bearing types [15]. An example is presented here. The calculations are carried out for a steel tank (tensile strength f_{yk} = 240 N/mm², weight of 2393 t) with constant wall thickness, firmly anchored to a reinforced concrete base plate (compression strength f_{ck} = 50 N/mm²) and filled with water. The geometry of the tank is illustrated in Fig. 3. The base plate is supported on nine seismic isolators. Two different types of bearings are investigated; their properties are given in Tab. 2. Fig. 4 shows the acceleration response spectrum of the seismic hazard zone, which is taken for the calculation. The velocity time history used for the calculation with the FSI-model is artificially generated from this spectrum. The calculations of the base isolated tanks are carried out for an elastic behavior of the tank structure itself and a damping of the fluid of 0.5%.
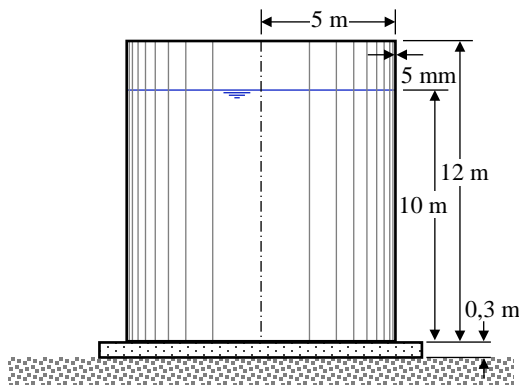
Fig. 3 – Geometry of the calculation example
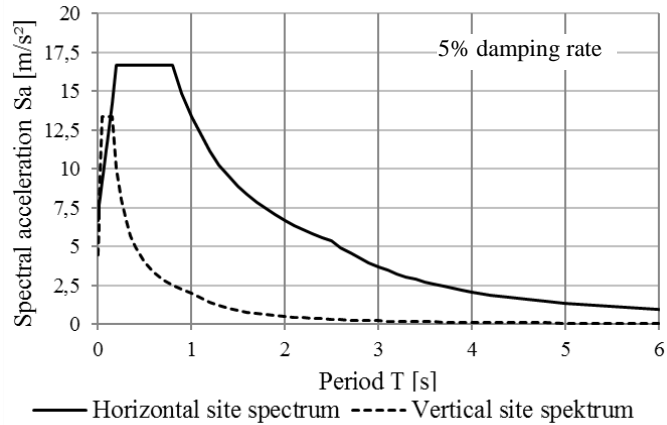
Fig. 4 – Acceleration response spectrum

Table 2 – Properties of the bearings

Elastomeric bearing with lead core		Friction pendulum bearing	
Initial stiffness K_1	7,18E+06 N/m	Yield displacement u_y	0,001 mm
Post yield stiffness K_2	5,52E+05 N/m	Radius for sliding R_{FPB}	7,1 m
Characteristic strength F_0	63E+03 N	Max. friction coefficient μ_{dyn}	8,7 %
Vertical compr. strength	1,67E+09 N/m	Diff. of friction coefficients	6,95 %
Vertical tensile strength	8,35E+08 N/m	Vertical load of the bearing V_L	9,24E+05 N

Fig. 5 shows the hysteretic behavior of the bearings in comparison to the bilinear idealization. For the two different bearing types, the numerical model simulates the idealized hysteresis accurately.

Because of the small but existing vertical flexibility of elastomeric bearings, tanks isolated with those bearings are vulnerable to so-called rocking effects. In Fig. 6, response time history of the vertical displacement of two opposed points of the tank bottom is presented. The vertical seismic excitation is subtracted. A difference in the vibration behavior of the tank can be observed. However, the resulting inclination of the tank is just a few millimeters, which does not affect the hydrodynamic pressure distribution of the isolated tank. The second conclusion deducted from the FSI-calculation is the following: Only the amplitude of the hydrodynamic pressure due to the horizontal component of the seismic excitation is affected from the base isolation. As a matter of fact, Fig. 7 shows the crucial pressure distribution for an angle of circumference θ=0° over the wetted tank height for for an excitation only in the vertical direction, considering the elastomeric bearings as well as rigid support conditions. It can be seen clearly, that the pressure distribution for the isolated tank is practically the same with that corresponding to a rigidly supported tank. The third noteworthy result is: The pressure distribution over height and circumference of the tank is identical to that pressure distribution of a rigidly supported tank. Fig. 8 illustrates this fact. Here, the well-known hydrodynamic pressure distribution [4], [5], [6], [8] over the tank
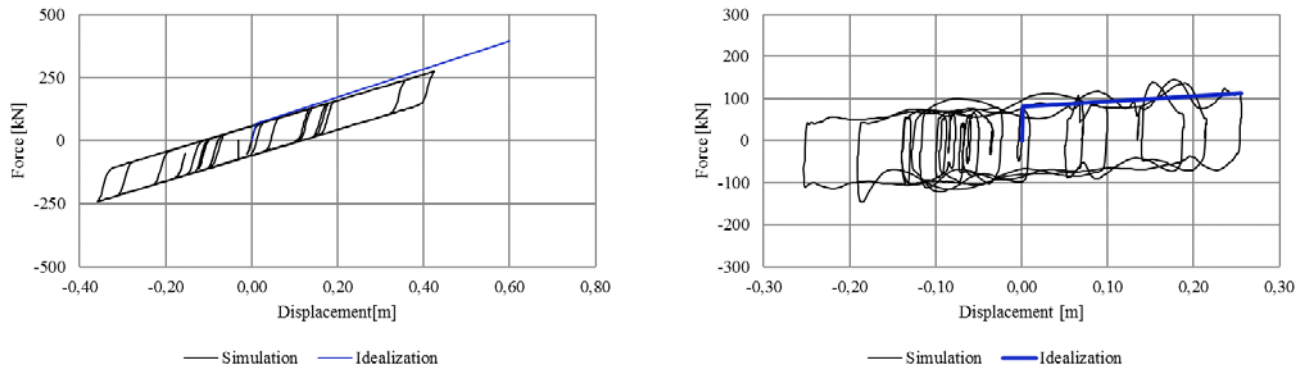
Fig. 5 – Idealized and calculated hysteresis of elastomeric bearing (left) and friction pendulum bearing (right)

height and circumference corresponding to the sinusoidal distribution of rigidly supported tanks is depicted. By utilizing these findings, a simplified mechanical model for isolated liquid storage tanks is subsequently derived.
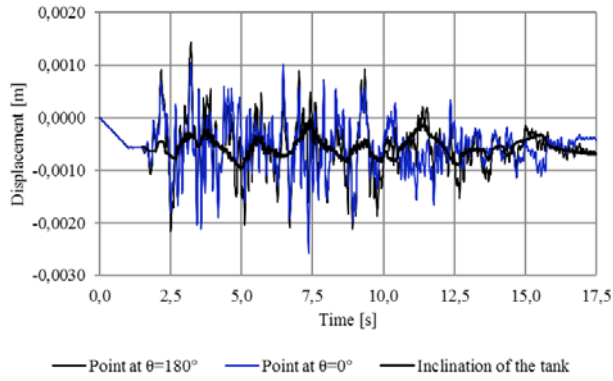
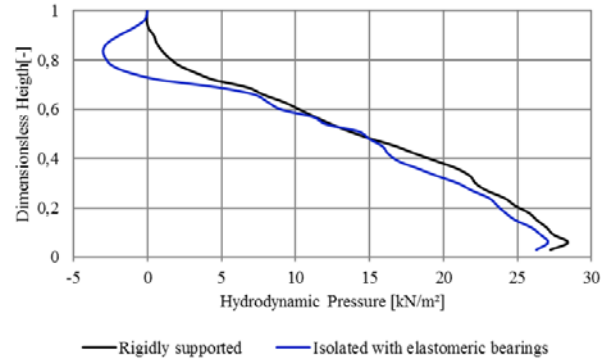Fig. 6 – Vertical displacement of the tank due to horizontal excitation

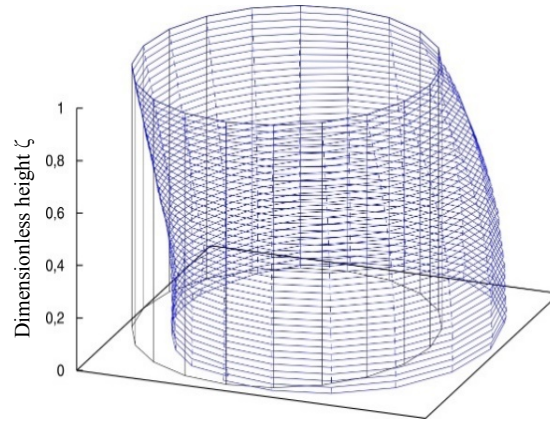Fig. 7 – Pressure distribution due to vertical seismic excitation

Fig. 8 – Qualitative pressure distribution due to horizontal and vertical seismic excitation of an isolated tank

3.5 Simplified mechanical model

The implementation takes place in several steps: First, with the aid of the added mass method presented in section 2, the normalized pressure components for a rigidly supported tank are determined. The integration of these provides the seismically induced masses, which are assembled into a mass oscillator (Fig. 9):

$$m_{i,1} = \int_0^H \int_0^{2\pi} \left[\bar{p}_{i,1}(\xi = 1, \zeta, \theta) \cdot cos(\theta) \right] \cdot R \, d\theta dz \tag{17}$$

$$m_{i,2} = \int_0^H \int_0^{2\pi} \left[\bar{p}_{i,2}(\xi = 1, \zeta, \theta) \cdot cos(\theta) \right] \cdot R \, d\theta dz \tag{18}$$

$$m_{c,1} = \int_0^H \int_0^{2\pi} \left[\bar{p}_{c,1}(\xi = 1, \zeta, \theta) \cdot cos(\theta) \right] \cdot R \, d\theta dz \tag{19}$$

In the integration a sinusoidal pressure distribution over the circumference of the tank is assumed, which is projected with $cos(\theta)$ to the excitation direction. The individual seismically activated masses are attached at the node 3 (impulsive mass of the first eigenmode), node 4 (impulsive mass of the second eigenmode) and node 5 (convective), the tank mass is concentrated at node 1. The stiffness of the impulsive and convective components related with each particular mass and its natural circular frequency ω (Eq. (2) and Eq. (4)) is obtained with the relationship $k = \omega^2 \cdot m$. As the behavior of the tank remains elastic only the fluid damping of 0.5% according to Eurocode 8 [9] is estimated. The properties of the seismic isolation are represented by a corresponding nonlinear element that is placed between nodes 1 and 2 (Fig. 10). A rheological element by combining springs and a friction element is used. The parameters of the bilinear hysteresis curve are the stiffness of the elastic and plastic range, K_1 and K_2, the yield force and the initial friction force F_0 accordingly.

The developed mass oscillator is employed to calculate the response acceleration of the tank in case of an isolated support. The load $a(t)$ is applied as a synthetically generated acceleration time history at node 2 of the system. With the absolute response accelerations of the individual masses determined, the normalized pressure components are scaled:

$$p_{i,1,iso}(\zeta,\theta) = a_{3,abs}^{max} \cdot \bar{p}_{i,1}(\zeta,\theta) \tag{20}$$

$$p_{i,2,iso}(\zeta,\theta) = a_{4,abs}^{max} \cdot \bar{p}_{i,2}(\zeta,\theta) \tag{21}$$

$$p_{c,1,iso}(\zeta,\theta) = a_{5,abs}^{max} \cdot \bar{p}_{c,1}(\zeta,\theta) \tag{22}$$

Here, $a_{3,abs}^{max}$ stands for the maximum absolute acceleration of node 3, $a_{4,abs}^{max}$ the one of node 4 and $a_{5,abs}^{max}$ the one of node 5. These three individual pressure components can be combined to the resulting pressure component of the isolated tank due to horizontal seismic excitation:

$$p_{h,iso}(\zeta,\theta) = p_{i,1,iso}(\zeta,\theta) + p_{i,2,iso}(\zeta,\theta) + p_{k,1,iso}(\zeta,\theta) \tag{23}$$

It has to be mentioned, that the maximum response acceleration at node 3, 4 and 5 appear at different time points. However, conducted parametric studies indicate that it is admissible to carry out the superposition of the components by considering their maximum values.

The combination with the non-scaled pressure due to vertical earthquake motion according to Eq. (8) is based on the 30% rule:

$$p_{iso,total}(\zeta) = p_{h,iso}(\zeta,\theta) \cdot \cos(\theta) + 0{,}3 \cdot p_{v,rigid}(\zeta) \tag{24}$$

Afterwards, the pressure components can be applied as static equivalent loads on a three-dimensional finite element model of the tank. This procedure allows the calculation of the stress state of a seismic isolated tank structure.

3.5 Results of the calculation with the simplified mechanical model in comparison to the FSI-calculation

On the basis of reference calculations for the tank described in section 3.3, the validity of the developed model is verified. The corresponding values for the establishment of the mass oscillator are listed in Tab. 3.

Table 3 – Parameter of the mass oscillator

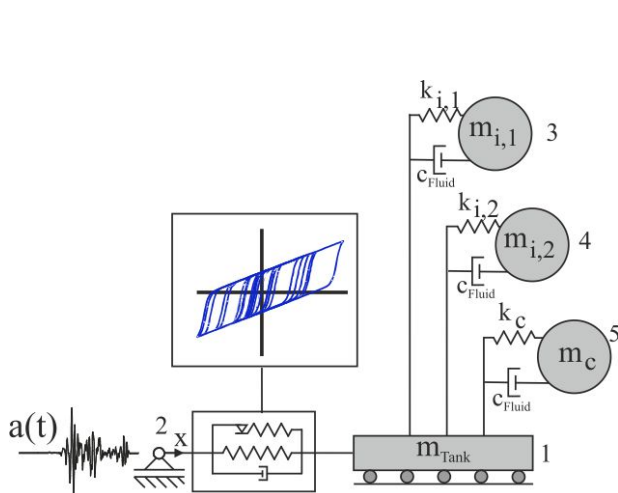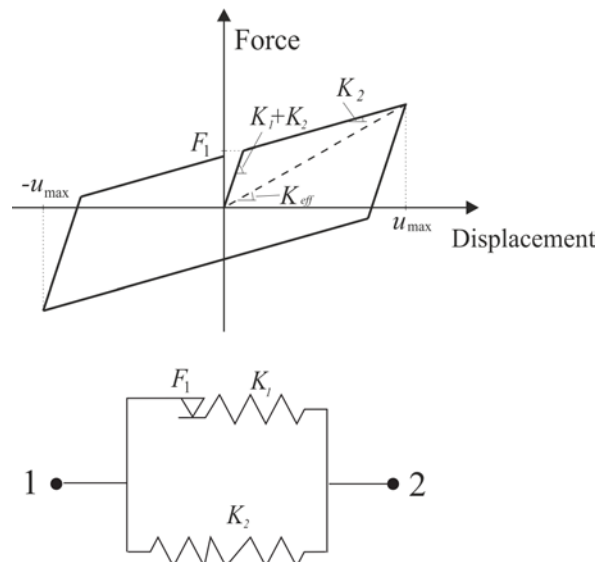| Tank structure	Friction pendulum bearing	Elastomeric bearing

Fig. 9 – Mass oscillator

Fig. 10 –Rheological element to simulate the nonlinear behavior of the base isolation

Mass $m_{i,1}$	538 t	Stiffness $k_{i,1}$	11,305E+08 N/m	Stiffness K_1	80,52E+06 N/m	Stiffness K_1	7,18E+06 N/m
Mass $m_{i,2}$	54 t	Stiffness $k_{i,2}$	6,248E+08 N/m	Stiffness K_2	0,13E+06 N/m	Stiffness K_2	0,55E+06 N/m
Mass $m_{c,1}$	357 t	Stiffness $k_{c,1}$	1,28E+06 N/m	Yield force F_0	80E+03 N	Yield force F_0	68E+03 N

The evaluation of the hysteresis curve demonstrates that the rheological model is able is to reproduce the hysteretic behavior of the seismic isolator (Fig. 11). The force-displacement curves correspond quite good to the FSI-calculation. The damping by energy dissipation is accordingly also well recorded in the simplified calculation. The relative displacements between foundation and tank structure and the maximum transmitted shear force show a very good agreement.

In Fig. 12 the hydrodynamic pressure of the rigidly supported tank following the calculation introduced in section 2 is presented. Additionally, the pressure of the isolated tank is shown regarding the calculation with the FSI-model and with the simplified approach. The pressure distribution of the calculation with the FSI model is presented for two different time points: The time point at which the maximum pressure acting on the lower part of the tank shell occurs, which corresponds to the maximum impulsive pressure, and additionally, the time point with the maximum pressure at the top of the tank, which corresponds to the maximum pressure due to sloshing of the liquid. As the both pressure components correspond to different Eigenfrequencies, as a matter of course their maxima occur within a time history analysis at different time points. First of all, Fig. 12 shows a significant decrease of the resulting hydrodynamic pressure in contrast to the rigidly supported tank, which results from the frequency shift and the increasing damping rate caused by the isolated support. Furthermore, the results concerning the isolated tank, show a satisfactory agreement between the investigated calculation schemes, even if the pressure calculated with the simplified model leads to a conservative design. However, this is believed to be justified for a simplified calculation approach.

Concerning the absolute horizontal displacement time history at the bottom of the tank, the results of the simplified mass oscillator are equal to the ones from the calculation with the FSI-model (Fig. 13). Thus, the expected displacements that pipe connections may charge, are well simulated.

Finally, the stress calculation is carried out by applying the pressure component (Eq. 24) as equivalent load on the "dry" shell of a 3D-finite-element model of the tank structure. Exemplarily, Fig. 14 shows the axial stress distribution of the tank regarding the calculation with the FSI-model and the introduced simplified approach. Conservative values of axial stresses, as expected because of higher pressure amplitudes, are computed with the aid of the simplified calculation scheme. However, the qualitative distribution of the two solutions is in good agreement.

4. Conclusion

The seismic excitation of rigidly supported liquid storage tanks activates hydrodynamic pressure components, which may lead to uneconomic wall thicknesses. A significant reduction of the seismic induced loads can be achieved by application of base isolations with elastomeric bearings or friction pendulum bearings. This paper introduces two calculation models for base-isolated tanks with different levels of accuracy. The simplified mechanical model is an equivalent mass oscillator, which is used for the calculation of modified hydrodynamic pressure components for the base isolated tank. The more sophisticated simulation model is realized with LS-DYNA©, which takes into account the fluid-structure interaction.

The results of both models show a satisfactory agreement. The proposed simplified model constitutes a handy computational tool for the assessment of the hydrodynamic pressure distribution along the tank wall height and over the circumference of a base isolated tank. Thus, the shell even of a base isolated tank can be designed with sufficient accuracy for the expected seismic load. Because of its simplicity, it is very suitable for practical applications and can be implemented in any software products that allow dynamic analysis.
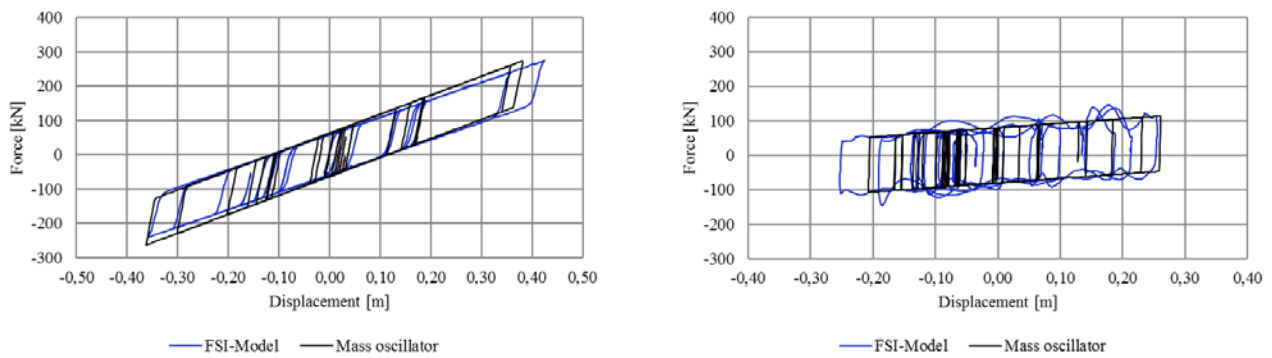
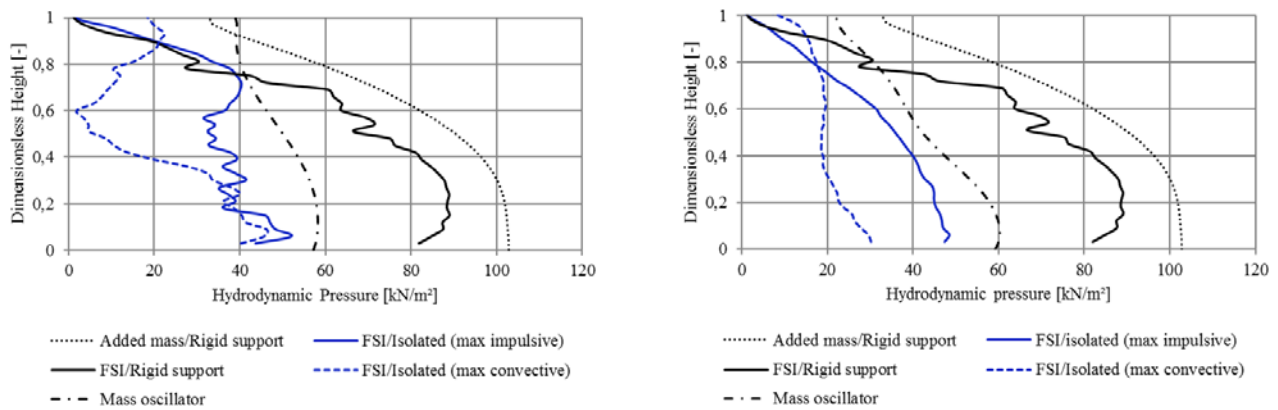Fig. 11 – Hysteresis curve (left: elastomeric bearing, right: friction pendulum bearing)

Fig. 12 – Pressure distribution at $\theta = 0°$ (left: elastomeric bearing, right: friction pendulum bearing)
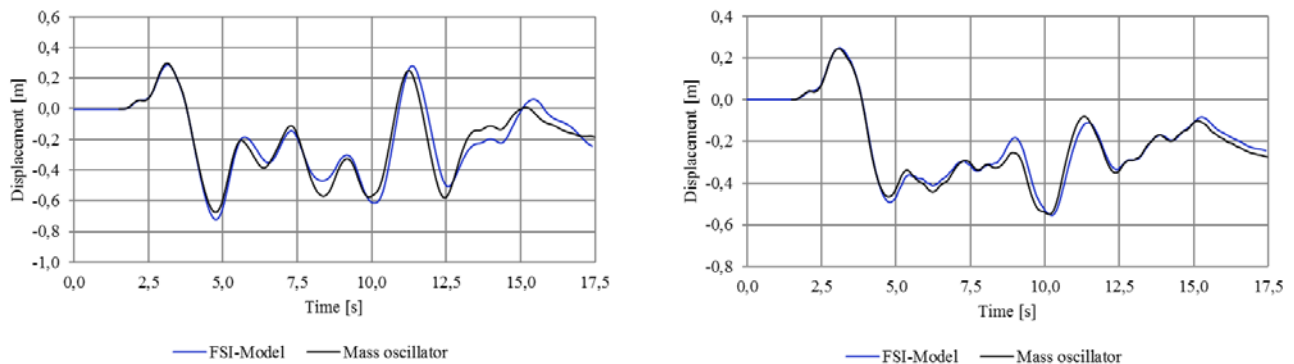

Fig. 13 – Horizontal Displacement of the tank bottom (left: elastomeric bearing, right: friction pendulum bearing)
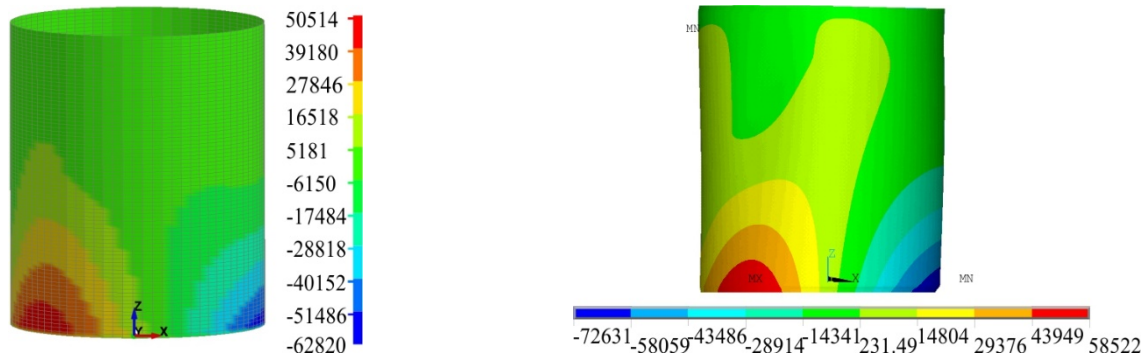
12

Fig. 14 – Axial stress distribution of the isolated tank, isolation with elastomeric bearings; left: FSI-model (time point of maximum compressive axial stress), right: simplified calculation approach

5. References

[1] Kelly TE (2001): Base Isolation of Structures – Design Guidelines. Holmes Consulting Group New Zealand.

[2] Mayes RL, Naeim F (2001): The Seismic Design Handbook, Chapter 14: Design of Structures with Seismic Isolation, Springer US, 2nd edition.

[3] Panchal VR, Soni DP (2014): Seismic behaviour of isolated fluid storage tanks: A-state-of-the-art review. *KSCE Journal of Civil Engineering,* **18** (4), 1097-1104.

[4] Haroun MA, Housner GW (1981). Seismic design of liquid storage tanks. *Journal of the Technical Council of ASCE* **197** 191-207.

[5] Veletsos AS (1974). Seismic Effects in Flexible Liquid Storage Tanks. Proceedings of the 5th World Conference on Earthquake Engineering.

[6] Fischer FD, Rammerstorfer FG, Scharf K (1991). Earthquake Resistant Design of Anchored an Unanchored Liquid Storage Tanks under Three Dimensional Earthquake Excitation. In: Schueller GI: Structural Dynamics, Springer, Berlin.

[7] Malhotra PK, Wenk T, Wieland M (2000). Simple Procedure for Seismic Analysis of Liquid Storage Tanks. *Structural Engineering International* **10** (3), 197-201.

[8] Meskouris K, Hinzen KG, Butenweg C, Mistler M (2011). Bauwerke und Erdbeben. Vieweg und Teubner, 3rd edition.

[9] DIN EN 1998-4 (2007). Eurocode 8: Design of structures for earthquake resistance – Part 4: Silos, tanks and pipelines. German Version, Deutsches Institut für Normung, Berlin.

[10] Mykoniou K (2015). Dynamic analysis of multiple liquid-storage tanks. Dissertation. RWTH Aachen University.

[11] Luft RW (1984). Vertical accelerations in pre-stressed concrete tanks. *Journal of Structural Engineering* **110**, 706-714.

[12] Tang Y (1986). Studies of dynamic response of liquid storage tanks. PhD Thesis, Rice University.

[13] Ozdemir Z, Souli M und Fahjan YM (2010). Application of Nonlinear Fluid-Structure-Interaction Methods to Seismic Analysis of Anchored and Unanchored Tanks. *Engineering Structures* **32**, 409–423.

[14] Maekawa A (2012). Recent Advances in Seismic Response Analysis of Cylindrical Liquid Storage Tanks. INTECH Open Access Publisher.

[15] Rosin J (2016). Seismische Auslegung von Tankbauwerken. Dissertation. RWTH Aachen University.

[16] Bouc R (1971). Modele Mathematique d'Hysteresis. *Acustica* **24**, 16–25.

[17] Wen YK (1976). Method of Random Vibration of Hysterestic Systems. *Journal of Engineering Mechanics Division* **102**, 249–263.

[18] Constantinou M, Mokha A Reinhorn A (1990). Teflon Bearing in Base isolation II - Modeling. *Journal of Structural Engineering* **116**, 455–474.

[19] Dimizas PC, Koumousis VK (2005). System Identification of Non-linear Hysteretic Systems with Application to Friction Pendulum Isolation Systems. 5th GRACM International Congress on Computational Mechanics.